



UNIVERSITÀ  
DEGLI STUDI  
DI PADOVA

*Università degli Studi di Padova*

*Padua Research Archive - Institutional Repository*

Mechanisms of HIV-1 Nucleocapsid Protein Inhibition by Lysyl-Peptidyl-Anthraquinone Conjugates

*Original Citation:*

*Availability:*

This version is available at: 11577/3217303 since: 2017-01-20T16:52:24Z

*Publisher:*

American Chemical Society

*Published version:*

DOI: 10.1021/acs.bioconjchem.5b00627

*Terms of use:*

Open Access

This article is made available under terms and conditions applicable to Open Access Guidelines, as described at <http://www.unipd.it/download/file/fid/55401> (Italian only)

(Article begins on next page)

# Mechanisms of HIV-1 Nucleocapsid Protein Inhibition by Lysyl-Peptidyl-Anthraquinone Conjugates

Alice Sosis,<sup>†</sup> Laura Sinigaglia,<sup>†</sup> Marta Cappellini,<sup>†</sup> Ilaria Carli,<sup>‡</sup> Cristina Parolin,<sup>‡</sup> Giuseppe Zagotto,<sup>†</sup> Giuseppina Sabatino,<sup>§</sup> Paolo Rovero,<sup>⊥</sup> Dan Fabris,<sup>||</sup> and Barbara Gatto<sup>\*,†</sup>

<sup>†</sup>Dipartimento di Scienze del Farmaco and <sup>‡</sup>Dipartimento di Medicina Molecolare, Università di Padova, 35122 Padova, Italy

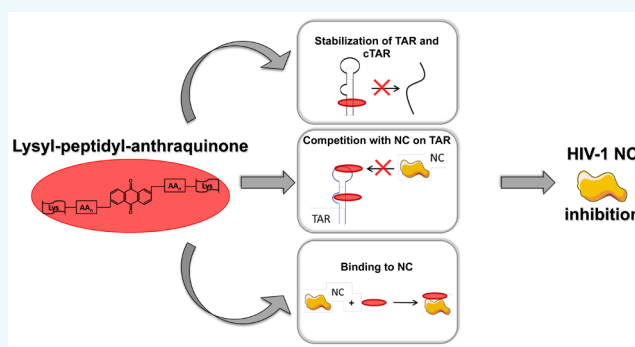
<sup>§</sup>Espikem SRL, Sesto Fiorentino, 50019 Firenze, Italy

<sup>⊥</sup>Dipartimento NeuroFarBa, Sezione di Scienze Farmaceutiche e Nutraceutica, Università di Firenze, 50121 Firenze, Italy

<sup>||</sup>Department of Chemistry, State University of New York, Albany, New York 12222, United States

## Supporting Information

**ABSTRACT:** The Nucleocapsid protein NCp7 (NC) is a nucleic acid chaperone responsible for essential steps of the HIV-1 life cycle and an attractive candidate for drug development. NC destabilizes nucleic acid structures and promotes the formation of annealed substrates for HIV-1 reverse transcription elongation. Short helical nucleic acid segments bordered by bulges and loops, such as the Trans-Activation Response element (TAR) of HIV-1 and its complementary sequence (cTAR), are nucleation elements for helix destabilization by NC and also preferred recognition sites for threading intercalators. Inspired by these observations, we have recently demonstrated that 2,6-disubstituted peptidyl-anthraquinone-conjugates inhibit the chaperone activities of recombinant NC in vitro, and that inhibition correlates with the stabilization of TAR and cTAR stem-loop structures. We describe here enhanced NC inhibitory activity by novel conjugates that exhibit longer peptidyl chains ending with a conserved N-terminal lysine. Their efficient inhibition of TAR/cTAR annealing mediated by NC originates from the combination of at least three different mechanisms, namely, their stabilizing effects on nucleic acids dynamics by threading intercalation, their ability to target TAR RNA substrate leading to a direct competition with the protein for the same binding sites on TAR, and, finally, their effective binding to the NC protein. Our results suggest that these molecules may represent the stepping-stone for the future development of NC-inhibitors capable of targeting the protein itself and its recognition site in RNA.



with the stabilization of TAR and cTAR stem-loop structures. We describe here enhanced NC inhibitory activity by novel conjugates that exhibit longer peptidyl chains ending with a conserved N-terminal lysine. Their efficient inhibition of TAR/cTAR annealing mediated by NC originates from the combination of at least three different mechanisms, namely, their stabilizing effects on nucleic acids dynamics by threading intercalation, their ability to target TAR RNA substrate leading to a direct competition with the protein for the same binding sites on TAR, and, finally, their effective binding to the NC protein. Our results suggest that these molecules may represent the stepping-stone for the future development of NC-inhibitors capable of targeting the protein itself and its recognition site in RNA.

## INTRODUCTION

HIV-1 Nucleocapsid protein (NC) is a small, highly basic protein of 55 amino acid residues, which mediates essential replication steps, such as strand transfers during reverse transcription of viral RNA and genome packaging during virion assembly.<sup>1–3</sup> Its structure is composed of a flexible 11-amino-acid N-terminus that includes four conserved basic residues (Lys3, Arg7, Arg10, and Lys11) and a core consisting of two zinc finger (ZF) domains.<sup>2,4</sup> The fact that ZF motifs are highly conserved and their mutations render the virus noninfectious limits the possibility that HIV-1 will be able to generate viable resistant strains, making NC a promising target for anti-HIV drug development.<sup>3,5–7</sup> The multifaceted activities enacted by NC originate from its nucleic acid-binding and chaperoning properties. Its interaction with cognate nucleic acids can induce transient melting of base-pairing, making previously paired strands available for reannealing in more thermodynamically stable structures.<sup>8–10</sup> The protein exhibits high affinity for single-stranded regions: unpaired nucleotides (e.g., bulges or small loops) in double-stranded stem structures are preferred

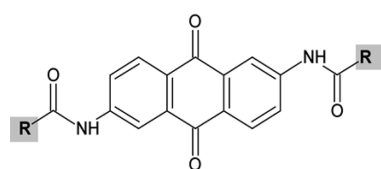
nucleation sites for helix destabilization, mediated by specific contacts with the ZF domains.<sup>11,12</sup> Additionally, numerous studies have shown that GNG sequences located in the apical loops of RNA hairpins constitute strong binding sites for the protein.<sup>13–16</sup> These studies have also highlighted the high flexibility and adaptability of NC to different types of nucleic acid substrates.<sup>4,13,15–18</sup>

An essential target of NC activity is the Trans-Activation Response element TAR, a stable stem-bulge-loop domain of the Long Terminal Repeat (LTR) region of genomic RNA, which is also required for Tat-mediated transcription.<sup>19</sup> Annealing of TAR to reverse-transcribed complementary DNA (cTAR) is an obligatory step of reverse transcription, which is mediated by NC.<sup>1,20</sup> Based on this premise, we hypothesized that small molecules capable of stabilizing these nucleic acid structures could interfere with the melting and annealing activities of NC,

Received: November 19, 2015

Revised: December 11, 2015

Published: December 14, 2015



compound	side chain R		
	AA <sub>1</sub>	AA <sub>2</sub>	AA <sub>3</sub>
1	βAla	K	
2	βAla	A	
3	βAla	A	K
4	βAla	G	K
5	G	A	K
6	G	G	K

**Figure 1.** Schematic structures of peptidyl-anthraquinone conjugates included in the study.

and we proved that disubstituted anthraquinone derivatives acting as threading intercalators were efficient NC inhibitors *in vitro*.<sup>21</sup> These compounds consist of a planar nucleus with the positively charged side chain substituents at the opposite sides of the ring system, such that one of the two substituents threads through the base pairs in the duplex to locate each chain in the nucleic acid grooves in the final intercalation complex.<sup>22</sup> The observed NC inhibition of disubstituted anthraquinones was enhanced when a basic amino acid (e.g., lysine, AA<sub>2</sub>) was the terminal anchor conjugated through a βAla spacer (AA<sub>1</sub>) to the 2 and 6 position of the ring system (compound 1, Figure 1);<sup>21</sup> preliminary experiments indicated in fact that NC inhibition was achieved also when the lysyl-peptidyl-chains were longer (compound 6, Figure 1).<sup>23</sup>

The aim of this work is to investigate the molecular mechanism(s) of lysyl-peptidyl-anthraquinones action in order to optimize NC inhibition. The present paper examines, in fact, a series of selected 2,6-disubstituted-anthraquinones with side chains different in length and composition, but characterized by an invariable N-terminal lysine (AA<sub>3</sub>) conjugated to the planar nucleus through amino acidic linkers (AA<sub>1</sub>, AA<sub>2</sub>) (compounds 3–6 in Figure 1, detailed in Supporting Information Figure S1). In previous studies focusing on G-quadruplex oligonucleotides, the same conjugates were described to exhibit preferential recognition of noncanonical conformations of nucleic acids over double stranded DNA.<sup>24</sup> However, their binding to dynamic DNA or RNA structures was not analyzed. Given their structure and the mentioned preliminary results, we verified whether these compounds have the potential to inhibit NC as demonstrated for 1.<sup>21</sup> Relative to our positive control 1, they place the electrostatic component of the side-chain in a more distal position from the intercalation moiety. Compound 2, lacking the amino side chain, was used as a negative control.


The inhibitory properties of these bioconjugates were tested *in vitro* by the concerted application of (i) fluorescence quenching assay (FQA), (ii) nucleocapsid annealing-mediated electrophoresis (NAME) assays, (iii) RNA footprinting, and (iv) direct infusion mass spectrometric (MS) analysis.

## RESULTS AND DISCUSSION

**Lysyl-Peptidyl-Anthraquinones Inhibit NC-Mediated Helix Destabilization of Folded TAR and cTAR.** A framework for understanding the *in vitro* effects of the selected anthraquinone conjugates on the NC-induced destabilization of TAR and cTAR structure was obtained by performing high throughput screening (HTS) experiments.<sup>21,25</sup> The apical portion of viral TAR domain was reproduced by a 29-nt RNA construct (that we called TAR) which combines a double-stranded stem with single-stranded loop and bulge regions. A complementary deoxy-oligonucleotide sequence (cTAR) was employed to mimic the DNA counterpart. Each construct was

properly double-labeled as previously described.<sup>21,26</sup> NC can induce melting of the lower half of the oligonucleotide stem, which increases the distance between fluorophore and quencher manifesting an increase of fluorescence. The inhibition of NC's helix destabilizing activity results in a quenching of fluorescence due to the proximity of the stem ends. After preliminary controls to ensure the absence of direct quenching activity by the compounds under investigation, their ability to inhibit stem melting was evaluated in the presence of recombinant full-length HIV-1 NC. Progressive increases of lysyl-peptidyl-anthraquinone amount allowed us to determine the concentration that induced 50% reduction of the stem-destabilizing activity of NC (i.e., IC<sub>50</sub>)<sup>21,25</sup> on TAR and cTAR (Table 1).

**Table 1.** Inhibition of NC-Induced Helix Destabilization (Melting) by Peptidyl-Anthraquinones

Compound –(side chain)	Helix destabilization 	
	IC <sub>50</sub> <sup>1</sup> (μM)	
	TAR	cTAR
1 –(βAla-K)	3.71±0.15 <sup>2</sup>	3.84±0.14 <sup>2</sup>
2 –(βAla-A)	49.3±1.44	43.1±1.43
3 –(βAla-A-K)	4.17±0.13	2.22±0.05
4 –(βAla-G-K)	4.49±0.31	2.07±0.02
5 –(G-A-K)	5.85±0.11	3.87±0.41
6 –(G-G-K)	2.60±0.04	2.28±0.22

<sup>1</sup>Data are averages ± SEM of three independent experiments.<sup>21</sup>

<sup>2</sup>Reported in ref 21.

The results summarized in Table 1 clearly show that, with the exception of the inactive compound 2, all tested lysyl-peptidyl conjugates inhibited NC-induced melting of TAR and of cTAR at micromolar concentrations. For 3–6, inhibition of stem-melting was achieved at slightly lower concentrations (IC<sub>50</sub>'s) when cTAR rather than TAR was considered. This observation is consistent with the typically greater destabilizing effects of NC on the cTAR's stem previously reported by other authors.<sup>27</sup> Among the lysyl-peptidyl-anthraquinones, compound 4 provided the highest level of inhibition in the series toward cTAR. Notably, compound 6 emerged from our analysis as the most potent NC inhibitor of the series toward TAR and, interestingly, it was more active than 1 in inhibiting NC-mediated stem melting activity on both TAR and cTAR constructs.

**Lysyl-Peptidyl-Anthraquinones Inhibit NC-Mediated Annealing of TAR to cTAR.** In addition to the effects of lysyl-

peptidyl-anthraquinones 3–6 on the stem-melting activity of NC, we investigated the effects on the strands-annealing properties by using the recently described nucleocapsid annealing mediated electrophoresis (NAME) assay.<sup>23</sup> This assay is based on the ability of NC or of its truncated form (NC<sub>12–55</sub> peptide) to mediate TAR/cTAR annealing, after efficient melting of the substrates' stems. The annealing process involves the specific interaction between apical loops of the two complementary sequences and proceeds through several intermediate steps to form the hybrid extended duplex TAR/cTAR.<sup>28</sup> The shorter NC<sub>12–55</sub> peptide lacks the basic N-terminal tail that is credited for the nonspecific nucleic binding properties, but retains both ZF motifs involved in the chaperoning activities. We tested both the protein and the peptide in the NAME assay: unlabeled prefolded TAR and cTAR were mixed with either full-length NC or NC<sub>12–55</sub> peptide in the presence of increasing ligand concentrations,<sup>23</sup> and the outcome of the annealing activity was observed by monitoring the formation of annealed TAR/cTAR heteroduplex by nondenaturing gel electrophoresis (see [Experimental Section](#)).


Anthraquinone derivatives 1–6 were tested in triplicate and a representative example of NAME assay obtained in the presence of 5 is reported in Figure S2 ([Supporting Information](#)). The progressive increase of peptidyl-anthraquinone conjugate concentration induced a decrease of the intensity of the band corresponding to the extended TAR/cTAR heteroduplex with a concomitant increase of the bands of free TAR and cTAR. The formation of intermediate complexes was also reduced in unison with the inhibition of extended heteroduplex, an outcome consistently observed in assays that used either full-length NC or NC<sub>12–55</sub> peptide. The formation of the extended heteroduplex was quantified as a function of inhibitor concentration in three independent analyses. The calculated IC<sub>50</sub> for the inhibition of the annealing activity promoted by full-length NC and NC<sub>12–55</sub> peptide are reported in [Table 2](#).

The peptidyl-anthraquinones 3–6 proved to be strong annealing inhibitors, with potency similar to that of acutissimins, natural products that bind and inhibit NC.<sup>26</sup> Annealing inhibition was achieved at lower concentrations in

experiments with the truncated NC<sub>12–55</sub> peptide, but the relative ranking of potency in the presence of full-length NC was comparable. Considering that truncation can limit the affinity of binding, but not the chaperoning activity, suggests a direct competition between the protein and the compounds for the same binding sites onto the nucleic acid structures. As expected, compound 2 lacking lysine was the least active in both type of tests. Compounds 3–5 are clearly more potent annealing inhibitors than 1, which contradicts the results of NC-induced melting experiments with TAR RNA ([Table 1](#)). It is also interesting to note that 6 was the most active inhibitor in the annealing test as well as in the NC-mediated stem melting activity toward TAR. Finally, we could observe that with the full-length protein the shorter G-spacer (AA<sub>1</sub> of the peptidyl chain in 5 and 6) is slightly better suitable than βAla to achieve NC inhibition.

**Lysyl-Peptidyl-Anthraquinones Inhibit TAR-Tat Complex Formation.** NC is not the only viral protein binding TAR: the HIV-1 trans-activator of transcription (Tat) has been recently described as a nucleic acids annealer, and shown to support NC in annealing reactions during reverse transcription.<sup>29,30</sup> Tat, in addition, is crucially required for efficient transcription of the integrated HIV viral genome<sup>31,32</sup> and its biological activity relies on its specific binding to TAR.<sup>33,34</sup> We therefore tested the ability of 1–6 to impair the complex formation between TAR RNA and a Tat peptide replicating the minimal amino acid sequence (48–57) necessary for TAR binding.<sup>35,36</sup> The protocol previously reported<sup>37,38</sup> is based on the use of TAR labeled with a quencher moiety and of Tat labeled with a fluorescent dye (see [Experimental Section](#)). The fluorophore emits efficiently when the peptide is free in solution, but its emission dramatically decreases when the complex is formed. Interference on Tat/TAR complex formation by the peptidyl-anthraquinone conjugate is clearly seen by the increase in fluorescence signal compared to what was observed in the peptide/nucleic acid titration curve, in the absence of inhibitors. These measures allowed us to determine the inhibition constants for each compound, as reported in [Table 3](#).

**Table 2. Peptidyl-Anthraquinones Inhibition of NC-Mediated Annealing**

Compound -(side chain)	Annealing activity 	
	Full length NC	NC <sub>12–55</sub>
1-(βAla-K)	44.5±0.69 <sup>2</sup>	34.7±0.68
2-(βAla-A)	>100	66.6±1.69
3-(βAla-A-K)	28.8±0.81	14.1±0.76
4-(βAla-G-K)	24.5±0.77	14.7±0.42
5-(G-A-K)	22.2±0.61	14.6±0.77
6-(G-G-K)	20.3±0.13	13.2±0.35

<sup>1</sup>Values are the mean ± SEM of three experiments performed in triplicate. <sup>2</sup>Reported in ref 21.

**Table 3. Inhibition of Tat/TAR Complex Formation by Peptidyl-Anthraquinones**

compound – (side chain)	K <sub>i</sub> <sup>a</sup> (μM)
1 – (βAla-K)	0.21 ± 0.01
2 – (βAla-A)	not active
3 – (βAla-A-K)	0.09 ± 0.01
4 – (βAla-G-K)	0.08 ± 0.01
5 – (G-A-K)	0.06 ± 0.01
6 – (G-G-K)	0.08 ± 0.02

<sup>a</sup>Values are the mean ± SEM of three experiments performed in triplicate.

Our results indicate that Tat/TAR complex formation was strongly inhibited by lysyl-peptidyl-anthraquinone. It is interesting to note that compounds 3–6 are clearly more potent Tat/TAR inhibitors than 1 ([Table 3](#)), as well as more potent NC-mediated annealing inhibitors than 1 as observed above ([Table 2](#)). In light of this dual activity, and of the fact that both NC and Tat proteins share TAR as substrate, our working hypothesis is that the in vitro activity of these longer conjugates relies on strongly targeting TAR RNA and that this effect is relevant for NC inhibition.



**Lysyl-Peptidyl-Anthraquinones Stabilize Stem-Loop Structured Nucleic Acids.** The peptidyl–anthraquinone conjugate **1** acting as a threading intercalator was able to stabilize the stem-loop structures of TAR and cTAR, and its NC inhibition was related to the stabilization of these dynamic structures.<sup>21</sup> We therefore decided to investigate the ability of **3–6** to bind and stabilize TAR and cTAR stem-loop structures by performing fluorescence quenching assay (FQA). Folded TAR and cTAR were analyzed in the absence/presence of compound, and the intercalation into nucleic acids was evidenced by an increase in melting temperature ( $T_m$ ). The results obtained from samples containing 1  $\mu$ M of nucleic acid substrate and 10  $\mu$ M of each compound are summarized in Figure 2.

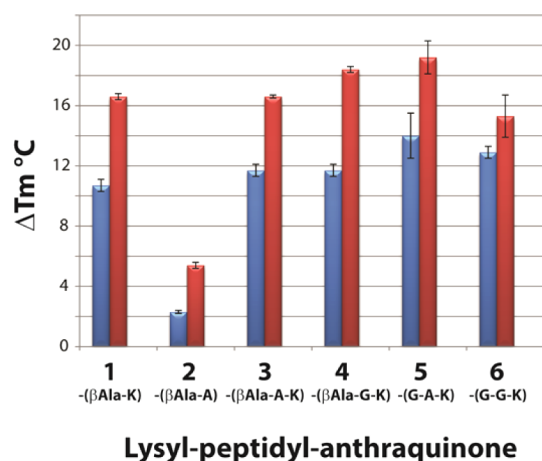


**Figure 2.** Variations of melting temperature ( $\Delta T_m$ ) manifested by TAR (blue) and cTAR (red) in the presence of peptidyl-anthraquinones. Side-chain sequences are in parentheses. Reported values are the mean  $\pm$  standard error of the mean (SEM) of triplicate experiments performed on samples containing 1  $\mu$ M of nucleic acid and 10  $\mu$ M of ligand. Reference  $T_m$  values for TAR and cTAR in the absence of ligand are 69.3 and 53.8  $^{\circ}$ C, respectively.

A marked increase of melting temperature of both RNA and DNA constructs was observed in the presence of compounds **3–6**, consistent with the hypothesis that these anthraquinones induce an efficient stabilization of nucleic acid double-helices. As demonstrated for **1**, the bioconjugates **3–6** efficiently stabilize TAR and cTAR substrates by intercalation into double-stranded nucleic acids and/or by stacking in the bulge/loop regions, as expected by threading intercalators.<sup>21,39</sup>

All tested compounds showed, not surprisingly, lower stabilization of the RNA compared to DNA construct, consistent with efficient intercalation of the planar anthraquinone ring into DNA, and in accordance with the lower inhibition of NC-induced stem melting on TAR over cTAR (Table 1). Stabilization was enhanced by the presence of lysine, as demonstrated by the lower  $\Delta T_m$  induced by compound **2** lacking the charged side-chains, confirming the influence of electrostatic interactions in nucleic acid binding. It is interesting to note that in the thermal melting experiment the ligands of the G-spacer series (**5** and **6**) stabilize the TAR construct slightly better than the compounds (**3–4**) bearing the  $\beta$ Ala linker, suggesting the possibility to modulate TAR recognition by fine-tuning the peptidyl chain substituents. Moreover, the enhanced TAR stabilization by **5** and **6** correlates with their higher NC-mediated annealing inhibition (Table 2) and with

their better effects on the Tat/TAR complex formation (Table 3).

These considerations prompted us to further analyze their TAR binding mode to prove our working hypothesis that the longer lysyl-bioconjugates efficiently target TAR RNA.

**Lysyl-Peptidyl-Anthraquinones Binding Sites on TAR RNA.** In order to investigate the location of putative binding sites of lysyl-peptidyl-anthraquinones on TAR, we set out footprinting experiments carried out treating radioactively labeled RNA, in the absence/presence of **5**, with ribonucleases having different specificities (Figure 2). We employed RNase T1 that cleaves single-stranded G; RNase A that hydrolyzes single-stranded C and U; and RNase V1 that preferentially attacks base-paired nucleotides.<sup>40</sup> Cleavage mixtures produced by increasing concentrations of enzyme were analyzed by denaturing gel electrophoresis. Footprinting data obtained in the absence/presence of compound **5** are reported in Figure 3.

In the absence of ligand, RNase T1 digestion produced preferential cleavage at G16 and, to a minor extent, G17 and G18 of the apical loop, which is consistent with their exposed placement in a single-stranded region. In contrast, the presence of ligand induced significant inhibition of nuclease activity in the same RNA region (see red box of Figure 3a, G16, G17, and G18 in the RNase T1 lanes). Comparable protection effects were also observed for the apical U15 upon treatment with RNase A (green box in Figure 3a, U15 in the RNase A lanes). At the same time, digestion by RNase V1 provided valuable insights into possible interactions involving base-paired nucleotides in the stem regions of the construct. Owing to its placement in a double-stranded region near the bulge, the G10 position was readily cleaved in the absence of compound **5**, but effectively protected by ligand binding (blue box in Figure 3a). A similar behavior was observed for the double-stranded A6 nucleotide lining the bulge (blue box in Figure 3a). The actual bulge nucleotides (i.e., U9, C8, and U7) were readily attacked by RNase A, but protected in the presence of **5** (green box in Figure 3a).

Inhibition of G10 and A6 hydrolysis was consistent with threading intercalation of the anthraquinone nucleus between the base pairs comprising these nucleotides and the adjacent ones in the surrounding stems (see cartoon in Figure 3b). Therefore, protection of unpaired bulge nucleotides (UCU, positions 7–9) could be explained by possible interactions with charged side-chains projected from the intercalated ligand. Interestingly, the sites protected by compound **5** correspond very well with the specific sites of destabilization of TAR RNA by NC, recently identified by McCauley et al.<sup>41</sup> The apical loop nucleotides G16, G17, G18, and U15 are placed farther away from the double-stranded stem of TAR and may not be within the reach of the side-chains of the intercalated ligand. Intercalators are, however, capable of binding also to single-stranded regions by establishing stacking interactions with exposed unpaired nucleobases.<sup>42</sup> This possibility could help explain the observed protection effects that we summarized in Figure 3b. The footprinting experiments with **5** on TAR RNA clearly identified two preferential binding sites located in the apical loop and bulge regions. It is striking to note that the unpaired bulge domain is the binding site of Tat protein on TAR,<sup>43,44</sup> while the weakly base-paired G bases on TAR hairpin<sup>41</sup> and the G-rich loop that cap TAR stem constitute the preferred nucleation sites of NC.<sup>13,14,16</sup> These results raised the possibility that such ligands may interfere directly with NC



occupied by ligand, which can lead to the accumulation of a 1:1 complex and disappearance of free unbound receptor before any 2:1 complex is detected. In Figure 4a, for example, this possibility was clearly incompatible with the simultaneous detection of both free TAR (i.e., [TAR - 7H]<sup>7-</sup>) and its 2:1 complex with species 5 (i.e., [TAR:2(5) - 7H]<sup>7-</sup>). When binding is cooperative, occupation of the first site translates into a significant increase of the probability of binding to the second one, which manifests in the absence of accumulation of 1:1 complex and simultaneous detection of both free and 2:1 complex. The pattern observed in Figure 4a did not support significant cooperativity, but was instead consistent with the presence of two independent binding sites with comparable affinities. Similar binding modes were detected for all the TAR complexes observed in the study. Interestingly, these data are in accordance with the footprinting analysis that revealed two preferential binding sites of 5 on TAR (Figure 3). Hence, a direct competition between the protein and compounds for the same binding sites on TAR structure constitutes a valid inhibition mechanism for lysyl-peptidyl-anthraquinones, but is not sufficient to resolve the observed differences in NC annealing inhibitory activity observed for 5 and 6 compared to 1 (Table 2).

**Direct Binding of Lysyl-Peptidyl-Anthraquinones to NC Protein.** The possibility that ligands may bind directly to NC could represent a valid explanation for the observed discrepancy. In order to test this hypothesis, we probed the ability of compounds 1, 5, and 6 to bind full-length NC. The outcome was monitored by ESI-MS determinations under conditions that have been proven to enable the detection of intact zinc-bound NC.<sup>49</sup> Accordingly, the analysis of protein sample in the absence of ligand afforded a mass of 6488.905 Da, which matched very closely the monoisotopic value of 6488.906 Da calculated from the sequence and including two Zn(II) ions. Representative spectra obtained in the presence of selected lysyl-peptidyl-anthraquinones are shown in Figure 5, while the observed masses are reported in Table S4 (Supporting Information).

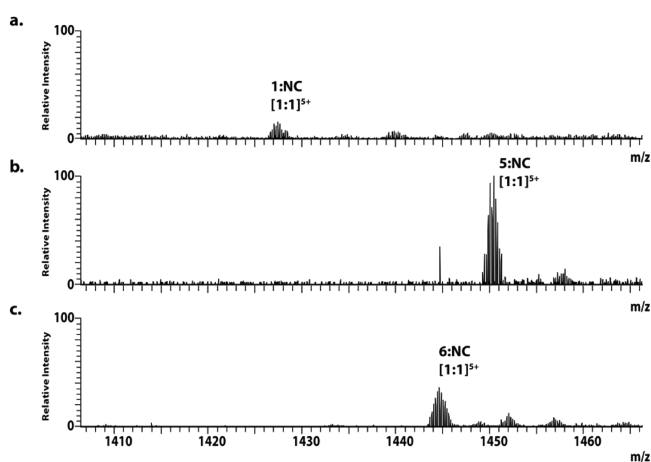


**Figure 5.** Representative ESI-MS spectra of NC samples in the presence of (a) 1-( $\beta$ Ala-K), (b) 5-(G-A-K), and (c) 6-(G-G-K). Each analysis was completed in positive ion mode on solutions containing 2  $\mu$ M of NC protein and 40  $\mu$ M of ligand (see Experimental Section). The observed binding stoichiometries are indicated in the figure. Weaker signals near the main peak are typical sodium and ammonium adducts. Only the region containing the complex is reported for clarity.

The results clearly show that the selected ligands are capable of binding to full-length NC to form stable 1:1 complexes. Given that these species were detected with the same charge state, an examination of their signal intensities allowed us to assume that compounds 5 and 6 do bind NC with higher affinity compared to 1.<sup>45,48</sup> This result matched very closely the data from the NAME assays, since 5 and 6 resulted in stronger NC inhibitors than 1 (Table 2). These observations revealed a direct correlation between side-chain composition, NC-binding, and inhibition. This is substantiated by the fact that the species with side-chains of extensive (5 and 6) and limited (1) size were at the opposite ends of the putative scale of NC binding and NC inhibitory activities. This suggests that the shorter derivative 1 could be better described as a nucleic acid intercalator, whose NC inhibition is due to the ability of stabilizing the nucleic acid substrates and to the competition for NC binding sites on TAR. The longer conjugates, placing lysine more distal from the planar moiety instead, include direct protein binding as an additional mechanism for achieving effective NC inhibition.

## CONCLUSIONS

Our study clearly demonstrates that lysyl-peptidyl-anthraquinone conjugates are strong in vitro inhibitors of HIV-1 NC activities. In analogy with 1, compounds 3–6 bind to and stabilize efficiently TAR and cTAR structures, with a better recognition of DNA over RNA construct. The results with NC showed that derivatives 3–6 display inhibition of the NC-mediated TAR and cTAR helix destabilization comparable to the reference 1; however, surprisingly, they show higher potency than 1 in inhibiting NC-mediated annealing activity. Interestingly, conjugates 3–6 are also more potent inhibitors of the Tat/TAR complex formation, displaying the same trend of activity identified for the NC-annealing inhibition. The slightly greater stabilization effect on TAR RNA exhibited by compounds 5 and 6, compared to the other conjugates, correlates with their slightly enhanced inhibition of both the NC-mediated annealing and the Tat/TAR complex formation, confirming the importance of TAR RNA in the elucidation of lysyl-peptidyl-anthraquinones inhibition mechanism. These considerations and the fact that both NC and Tat proteins share TAR RNA as nucleic acid substrate, highlight the critical role of TAR in the inhibition mechanism of the tested conjugates. For this reason, we further analyzed their interactions with TAR RNA. An important clue was provided by RNA footprinting analysis, which identified apical loop and bulge regions as putative ligand sites onto TAR. These regions correspond respectively to the typical single-stranded structures preferred by NC binding<sup>13,15</sup> and to the binding site of Tat on TAR.<sup>43,44</sup> Therefore, it is very likely that ligands compete with protein binding to the RNA substrate, a hypothesis supported by the recent data on NC binding to TAR RNA.<sup>41</sup> We further analyzed the direct binding of lysyl-peptidyl-anthraquinones with TAR construct by ESI-MS and identified the coexistence of two independent binding sites on TAR sharing similar affinities and negligible cooperativity, which confirm footprinting data. Finally, our study demonstrates that longer conjugates can bind directly to NC, which advances protein binding as another additional component of their overall inhibitory activity. The structural determinants of the affinity of these derivatives toward NC are not well understood and will require further investigation.



Hence, we demonstrate that at least three combined mechanisms are contributing simultaneously to the overall NC inhibitory activity of this class of conjugates. The inhibitory activity of lysyl-peptidyl-anthraquinone conjugates on NC and Tat opens the possibility to consider them as multitarget inhibitors, able to interfere not only with NC-mediated reactions during reverse transcription, but also with the Tat-mediated transcription process, resulting eventually in the impairment of the viral replicative cycle at multiple steps. Therefore, our study indicates that the development of peptidyl bioconjugates for targeting RNA stem-loop structures alone, or in the context of their biologically relevant complexes, is certainly a viable strategy in the search for new molecules against druggable viral targets.

## ■ EXPERIMENTAL SECTION

**Materials.** Anthraquinones were synthesized as reported.<sup>24</sup>

All oligonucleotides were synthesized by Metabion International AG (Martinsried, Germany) and stored at  $-20\text{ }^{\circ}\text{C}$  in 10 mM Tris-HCl, pH 7.5. Dilutions were made in DEPC-treated water (Ambion). TAR is the 29-mer RNA sequence 5'-GGCAGAUCUGAGCCUGGGAGCUCUCUGCC-3' and cTAR is its DNA complementary sequence 5'-GGCAGAGAGCTCCCAGGCTCAGATCTGCC-3'. When specified, TAR and cTAR were labeled at 5'- and 3'-ends, respectively, by the fluorophore 5-carboxyfluorescein (FAM) and the dark quencher 4-(4'-dimethylaminophenylazo)benzoic acid (Dabcyl).

The full-length recombinant NC protein was obtained as reported.<sup>47</sup> The protein concentration was determined on a UV-vis Spectrophotometer Lambda 20, PerkinElmer, using an extinction coefficient at 280 nm of  $6410\text{ M}^{-1}\text{ cm}^{-1}$ .

**Solid-Phase Synthesis of NC<sub>12-55</sub> Peptide.** The NC<sub>12-55</sub> peptide was synthesized using a fully automated peptide synthesizer at room temperature on 100 mg of Nova Syn TGA Asn(Trt) resin (loading 0.20 mmol/g). N-Fmoc deprotection was performed in two stages using piperidine-DMF 40% for 2 min followed by piperidine-DMF 20% for 10 min. The resin was then washed with DMF. Coupling reactions were performed using N-Fmoc amino acids (5 equiv), TBTU (5 equiv) in DMF, and DIPEA (10 equiv) in NMP. All couplings were performed for 20 min. After each coupling the resin was washed with DMF (4 $\times$ ). At the end the resin was washed with DCM (3 $\times$ ) and dried. Peptide cleavage from the resin and deprotection of the amino acids side chains were carried out for 3 h at room temperature with Reagent K (TFA 94%, anisole 2%, Phenol 2%, EDT 2%, H<sub>2</sub>O 2%). The crude products were precipitated with diethyl ether, collected by centrifugation, dissolved in H<sub>2</sub>O, and lyophilized. The products were characterized by RP-HPLC ESI-MS (Waters Alliance 2695 apparatus equipped with a diode array detector) using a Phenomenex Kinetex C-18 column 2.6  $\mu\text{m}$  (100  $\times$  3.0 mm) 0.6 mL/min. The solvent systems used were: A (0.1% TFA in H<sub>2</sub>O Milli-Q) and B (0.1% TFA in CH<sub>3</sub>CN); with different gradients at 0.6 mL/min in 5 min. The NC<sub>12-55</sub> peptide was resuspended in Tris-HCl 10 mM pH = 7.5 and stored at  $-20\text{ }^{\circ}\text{C}$  and added of 2 equiv of zinc before use. The peptide concentration was determined on a UV-vis Spectrophotometer Lambda 20, PerkinElmer, using an extinction coefficient at 280 nm of  $5700\text{ M}^{-1}\text{ cm}^{-1}$ .

**Inhibition of NC-Mediated Destabilization of TAR and cTAR Stem.** The high throughput screening was performed to identify inhibitors of NC chaperone activity on both TAR and

cTAR as previously described.<sup>21</sup> We used a microplate reader VictorIII (PerkinElmer) with 485 and 535 nm as excitation and emission wavelengths. 5'-FAM and 3'-DAB modified TAR or cTAR (each 1  $\mu\text{M}$ ) were folded in TNMg (10 mM Tris-HCl, 20 mM NaCl, 1 mM Mg(ClO<sub>4</sub>)<sub>2</sub>, pH 7.5): the oligonucleotides were denatured at 95  $^{\circ}\text{C}$  for 5 min and then left to cool to room temperature in order to assume their stem-bulge-loop structure. cTAR or TAR was then diluted to 0.1  $\mu\text{M}$  in TN (10 mM Tris-HCl, 20 mM NaCl pH 7.5). Increasing concentrations of compound (0, 0.1, 0.5, 1, 5, 10, 50, 100  $\mu\text{M}$  final) were incubated with 0.1  $\mu\text{M}$  cTAR or TAR in each well. Finally, NC 0.8  $\mu\text{M}$  (molar ratio oligos/NC = 1/8) was added to each sample. The plate was read three times with a delay of 1 min one reading from the other. The experimental data were fitted as reported and the IC<sub>50</sub> value was calculated for each compound.<sup>21</sup> Each experiment was performed in triplicate to calculate a standard deviation of the IC<sub>50</sub> value.

**Inhibition of TAR/cTAR Annealing by Anthraquinones.** Nucleocapsid annealing mediated electrophoresis (NAME) assay was used to investigate the ability of compounds to impair the biological activity of the full length NC protein and of the truncated NC<sub>12-55</sub> peptide, monitoring the annealing of TAR with cTAR.<sup>23</sup> TAR, cTAR, and the hybrid TAR/cTAR (each 1  $\mu\text{M}$ ) each folded in TNMg (10 mM Tris-HCl, 20 mM NaCl, 1 mM Mg(ClO<sub>4</sub>)<sub>2</sub>, pH 7.5) were used as controls: the oligonucleotides were denatured at 95  $^{\circ}\text{C}$  for 5 min and then left to cool to room temperature in order to assume their stem-bulge-loop (TAR and cTAR) or double-stranded (hybrid TAR/cTAR) structure. To evaluate the inhibition of NC- or NC<sub>12-55</sub>-mediated TAR/cTAR hybrid formation, TAR (1  $\mu\text{M}$ ), and cTAR (1  $\mu\text{M}$ ) were folded separately as described above, individually incubated with increasing concentrations of compound (each oligo with 0, 1, 10, 50, 100  $\mu\text{M}$  compound concentrations) for 15 min at room temperature, mixed together, added to NC or NC<sub>12-55</sub> solution (8  $\mu\text{M}$ , oligos/protein or oligos/peptide = 1/8) and then incubated for other 15 min at room temperature. To the samples were added Gel Loading Buffer containing SDS (GLB<sub>SDS</sub>: 100 mM Tris-HCl, 4 mM EDTA, 50% w/v glycerol, 2% w/v SDS, 0.05% w/v bromophenol blue), held on ice, and finally resolved on a 12% native PAGE (Acrylamide:Bis-(acrylamide) = 19:1), run in TBE buffer (89 mM Tris, 89 mM boric acid and 2 mM EDTA, pH 8) for 3 h at 200 V. After electrophoresis, nucleic acids on the gel were stained with SybrGreen II and detected on a Geliance 600 Imaging System (PerkinElmer). The IC<sub>50</sub> (concentration of the compound required to inhibit the hybrid formation by half) was calculated by the quantification (using GeneTools software from PerkinElmer) of the percentage of the hybrid formation.<sup>21</sup>

**Inhibition of Tat/TAR Complex Formation by Anthraquinones.** The effect of peptidyl-anthraquinone conjugates on the Tat/TAR complex was evaluated using a FRET-based competition assay, as previously described.<sup>37,38</sup> The peptide sequence corresponding to the minimal amino acid sequence (48-57; GRKKRRQRRR) necessary for TAR binding was labeled with fluorescein (FAM) at its N-terminus and the 29-nt TAR was labeled at its 3' end with a Dabcyl moiety (dark quencher). Titrations of labeled Tat/TAR in the presence of anthraquinones were made in triplicates in a 96-well plate reader (Victor III, PerkinElmer); the FAM-labeled Tat was excited at 490 nm and the emission was recorded at 535 nm. The plates were assembled with 190  $\mu\text{L}$  of a solution containing 10 nM FAM-peptide in TNMg (Tris 10 mM, pH 7.5,



Mg(ClO<sub>4</sub>)<sub>2</sub> 1 mM, NaCl 20 mM, 0.01% Triton X-100), in the presence of a fixed amount of each compound (10 μM). Fluorescence intensities in the presence of increasing concentrations of DabcyL-TAR were measured and curves were fitted to obtain *K<sub>i</sub>* values. A preliminary determination of the spectral parameters of all quinolones allowed us to exclude optical interferences with fluorescein-peptide signal at the conditions of the assay.

**TAR and cTAR Stabilization by Anthraquinones.** The ability of each compound to interact with the TAR and cTAR structures was analyzed by fluorescence quenching assay (FQA), measuring the increase of melting temperature of the oligonucleotide in the presence of anthraquinones. Each oligo was folded at 10 μM in TNMg (10 mM Tris-HCl, 20 mM NaCl, 1 mM Mg(ClO<sub>4</sub>)<sub>2</sub>, pH 7.5) and then diluted to 1 μM concentration in ETN (1 mM EDTA, 10 mM Tris HCl, 20 mM NaCl, pH 7.5). In each microplate well the nucleic acid solutions were mixed with the anthraquinone solution to the final concentration of 1 and 10 μM. Nucleic acid solutions without compounds were used to measure the reference value for *T<sub>m</sub>*. The temperature was increased from 25 to 99 °C in 1 h (0.02 °C/s) to promote the thermal denaturation of the oligonucleotides, while the emission fluorescence (at 510 nm) was monitored (30 acquisitions per °C). The analysis was performed using the LightCycler480 II (Roche). The *T<sub>m</sub>* value was mathematically derived from the thermal denaturing profile using LC480 software.  $\Delta T_m$  was calculated using the following equation:  $\Delta T_m = T_{m2} - T_{m1}$ , where *T<sub>m2</sub>* and *T<sub>m1</sub>* are the *T<sub>m</sub>* values measured testing the oligonucleotides in the presence and in the absence of compound, respectively.

**Identification of Lysyl-Peptidyl-Anthraquinones Binding Sites on TAR.** Enzymatic RNase footprinting was employed to identify TAR regions involved in the binding of anthraquinone conjugates. TAR was 5'-radioactively labeled using T4 polynucleotide kinase (T4 PNK, Ambion, Applied Biosystems, TX, USA) in the presence of [ $\gamma$ -<sup>32</sup>P] ATP (3000 Ci/mmol, PerkinElmer, MA, USA) following manufacturer's instructions. The analysis of TAR structure was performed both in the absence and in the presence of 5 and the comparison of the two different patterns allowed the identification of the TAR regions involved in the binding. TAR structure analysis was performed using 0.2 μg of TAR added of Structure Buffer (10 mM Tris pH 7, 0.1 M KCl, 10 mM MgCl<sub>2</sub>). TAR was then denatured at 95 °C for 5 min and left to cool to room temperature in order to assume its stem-bulge-loop structure. To the samples was added 5 μL of compound (final concentration 300 μM) or DEPC-treated H<sub>2</sub>O. After 15 min at room temperature, to the samples was added 2 μL of tRNA (2 μg/μL) and finally to each sample tube was added a different RNase. RNA samples were digested with three sequential 10-fold dilutions of each ribonuclease starting from RNase T1 1 U/μL (Ambion), RNase V1 0.1 U/μL (Ambion), and RNase A 1 μg/mL (Ambion). The samples not treated with RNases were used as control. After 3 min incubation, the reactions were stopped using 5 μL of denaturing Gel Loading Buffer (95% formamide, 18 mM EDTA, 0.025% SDS, xylene cyanol and bromophenol blue, from Ambion). The alkaline hydrolysis of TAR was performed adding 1.5 μL of tRNA (2 μg/μL) to 0.1 μg of TAR in a final volume of 15 μL in the Hydrolysis Buffer (50 mM NaCO<sub>3</sub>, 1 mM EDTA, pH 9.2). Samples were heated to 95 °C for 5 min and the reaction was stopped putting the samples on ice and adding 5 μL of denaturing Gel Loading Buffer (GLB<sub>D</sub>: 95% formamide, 18 mM EDTA, 0.025% SDS,

0.05% xylene cyanol and 0.05% bromophenol blue, from Ambion). All samples were heated for 5 min at 95 °C, put on ice, and finally resolved on a sequencing denaturing PAGE (20% polyacrylamide gel with 7 M urea) for 1.5 h in TBE buffer (89 mM Tris, 89 mM Boric acid, and 2 mM EDTA, pH 8) at 95 W. After the run, the gel was autoradiographed (with Hyperfilm MP, Amersham film, and intensifying screens, Amersham) for 1 day and was then developed with developing and fixing buffers (Kodak).

**Analysis of Peptidyl-Anthraquinones Binding to TAR.** TAR was folded in 150 mM ammonium acetate (pH 7.5) containing 1 μM MgCl<sub>2</sub>: the oligonucleotide was denatured at 95 °C for 5 min and then left to cool to room temperature in order to assume its stem-bulge-loop structure. Before mixing with compounds, folded TAR was filtered by using centrifugal filters 3K NMWL (Millipore Corporation, MA, USA) to lower the presence of magnesium salts that can adversely interfere with ESI performance. Samples for the binding studies were prepared by mixing appropriate volumes of folded TAR (1 μM final) with each compound in 150 mM ammonium acetate (pH 7.5). The final mixtures contained up to a 10:1 lysyl-peptidyl-anthraquinone/oligo molar ratio. To ensure the binding equilibrium in solution, samples were incubated for 15 min at room temperature before the analysis. Control experiments were performed by using a solution of TAR (1 μM final) in 150 mM ammonium acetate, and solutions of each compound (10 μM final) in 150 mM ammonium acetate. All samples were analyzed in negative ion mode by direct infusion electrospray ionization (ESI) on a Thermo Fisher Scientific (West Palm Beach, CA) LTQ-Orbitrap Velos mass spectrometer. The analyses were performed in nanoflow ESI mode by using quartz emitters produced in-house by a Sutter Instruments Co. (Novato, CA) P2000 laser pipet puller. Up to 6 μL of sample was loaded onto each emitter by using a gel loader pipet tip. A stainless steel wire was inserted in the back-end of the emitter and used to supply an ionizing voltage ranged around 0.8–1.0 kV. Source temperature and desolvation conditions were adjusted to decrease the incidence of salt adducts, with typical source temperature of 200 °C. Data were processed by using Xcalibur 2.1 software (Thermo Scientific).

**Analysis of 1, 5, and 6 Lysyl-Peptidyl-Anthraquinones Binding to NC.** Samples for the binding studies were prepared by mixing appropriate volumes of stock solution of the full length NC (2 μM final) with each compound in 150 mM ammonium acetate (pH 7.5). The final mixtures contained up to a 20:1 compound/NC molar ratio, which allowed the detection of anthraquinones binding to the protein. In order to ensure the binding equilibrium in solution before analysis, the samples were incubated for 15 min at room temperature. We performed control experiments using a solution of NC protein in 150 mM ammonium. All samples were analyzed in positive ion mode by direct infusion electrospray ionization (ESI) on a Thermo Fisher Scientific (West Palm Beach, CA) LTQ-Orbitrap Velos mass spectrometer. The analyses were performed as previously described for the ESI-MS binding analysis of lysyl-peptidyl-anthraquinones to TAR.

## ■ ASSOCIATED CONTENT

### 📄 Supporting Information

The Supporting Information is available free of charge on the ACS Publications website at DOI: 10.1021/acs.bioconjchem.5b00627.

Figure S1: Structure of lysyl-peptidyl-anthraquinone conjugates. Figure S2: NAME assay: inhibition of TAR/cTAR annealing by lysyl-peptidyl-anthraquinone. S. Table S1: Monoisotopic mass (Da) of lysyl-peptidyl-anthraquinone:TAR complexes by ESI-MS analysis in negative ion mode. Table S2: Average mass (Da) of lysyl-peptidyl-anthraquinone:NC complexes by ESI-MS analysis. (PDF)

## AUTHOR INFORMATION

### Corresponding Author

\*E-mail: [barbara.gatto@unipd.it](mailto:barbara.gatto@unipd.it). Phone: +39 049 827 5717. Fax: +39 049 827 5366.

### Notes

The authors declare no competing financial interest.

## ACKNOWLEDGMENTS

B.G. thanks the financial support by Ministero degli Affari Esteri e Cooperazione Internazionale (DRPG, Grant: PGR00171) and by MIUR (Grant PRIN: 2010W2KM5L\_006).

## ABBREVIATIONS

HIV, Human Immunodeficiency Virus; NC, Nucleocapsid protein; TAR, Trans-Activation Response element; cTAR, DNA sequence complementary to TAR; ZF, zinc fingers; AA, amino acid; FQA, Fluorescence Quenching Assay; NAME, Nucleocapsid Annealing-Mediated Electrophoresis; HTS, High Throughput Screening; IC<sub>50</sub>, 50% inhibitory concentration; Tat, trans-activator of transcription; T<sub>m</sub>, melting temperature; RNase, ribonuclease; SDS, Sodium Dodecyl Sulfate; EDTA, ethylenediaminetetraacetic acid; PAGE, PolyAcrylamide Gel Electrophoresis

## REFERENCES

- (1) Guo, J., Henderson, L. E., Bess, J., Kane, B., and Levin, J. G. (1997) Human immunodeficiency virus type 1 nucleocapsid protein promotes efficient strand transfer and specific viral DNA synthesis by inhibiting TAR-dependent self-priming from minus-strand strong-stop DNA. *J. Virol.* **71**, 5178–88.
- (2) Levin, J. G., Guo, J., Rouzina, I., and Musier-Forsyth, K. (2005) Nucleic acid chaperone activity of HIV-1 nucleocapsid protein: critical role in reverse transcription and molecular mechanism. *Prog. Nucleic Acid Res. Mol. Biol.* **80**, 217–86.
- (3) Darlix, J. L., Garrido, J. L., Morellet, N., Mely, Y., and de Rocquigny, H. (2007) Properties, functions, and drug targeting of the multifunctional nucleocapsid protein of the human immunodeficiency virus. *Adv. Pharmacol.* **55**, 299–346.
- (4) Morellet, N., Jullian, N., De Rocquigny, H., Maigret, B., Darlix, J. L., and Roques, B. P. (1992) Determination of the structure of the nucleocapsid protein NCp7 from the human immunodeficiency virus type 1 by 1H NMR. *EMBO J.* **11**, 3059–65.
- (5) de Rocquigny, H., Shvadchak, V., Avilov, S., Dong, C. Z., Dietrich, U., Darlix, J. L., and Mely, Y. (2008) Targeting the viral nucleocapsid protein in anti-HIV-1 therapy. *Mini-Rev. Med. Chem.* **8**, 24–35.
- (6) Mori, M., Kovalenko, L., Lyonnais, S., Antaki, D., Torbett, B. E., Botta, M., Mirambeau, G., and Mely, Y. (2015) Nucleocapsid Protein: A Desirable Target for Future Therapies Against HIV-1. *Curr. Top. Microbiol. Immunol.* **389**, 53–92.
- (7) Garg, D., and Torbett, B. E. (2014) Advances in targeting nucleocapsid-nucleic acid interactions in HIV-1 therapy. *Virus Res.* **193**, 135–43.
- (8) Mougel, M., Houzet, L., and Darlix, J. L. (2009) When is it time for reverse transcription to start and go? *Retrovirology* **6**, 24.
- (9) Thomas, J. R., and Hergenrother, P. J. (2008) Targeting RNA with small molecules. *Chem. Rev.* **108**, 1171–224.
- (10) Rajendran, A., Endo, M., Hidaka, K., Tran, P. L., Mergny, J. L., Gorelick, R. J., and Sugiyama, H. (2013) HIV-1 nucleocapsid proteins as molecular chaperones for tetramolecular antiparallel G-quadruplex formation. *J. Am. Chem. Soc.* **135**, 18575–85.
- (11) Turner, K. B., Hagan, N. A., and Fabris, D. (2007) Understanding the isomerization of the HIV-1 dimerization initiation domain by the nucleocapsid protein. *J. Mol. Biol.* **369**, 812–28.
- (12) Mirambeau, G., Lyonnais, S., and Gorelick, R. J. (2010) Features, processing states, and heterologous protein interactions in the modulation of the retroviral nucleocapsid protein function. *RNA Biol.* **7**, 724–34.
- (13) Amarasinghe, G. K., De Guzman, R. N., Turner, R. B., Chancellor, K. J., Wu, Z. R., and Summers, M. F. (2000) NMR structure of the HIV-1 nucleocapsid protein bound to stem-loop SL2 of the psi-RNA packaging signal. Implications for genome recognition. *J. Mol. Biol.* **301**, 491–511.
- (14) Hagan, N. A., and Fabris, D. (2007) Dissecting the protein-RNA and RNA-RNA interactions in the nucleocapsid-mediated dimerization and isomerization of HIV-1 stemloop 1. *J. Mol. Biol.* **365**, 396–410.
- (15) Bazzi, A., Zargarian, L., Chaminade, F., Boudier, C., De Rocquigny, H., Rene, B., Mely, Y., Fosse, P., and Mauffret, O. (2011) Structural insights into the cTAR DNA recognition by the HIV-1 nucleocapsid protein: role of sugar deoxyriboses in the binding polarity of NC. *Nucleic Acids Res.* **39**, 3903–16.
- (16) Goudreau, N., Hucke, O., Faucher, A. M., Grand-Maitre, C., Lepage, O., Bonneau, P. R., Mason, S. W., and Titolo, S. (2013) Discovery and structural characterization of a new inhibitor series of HIV-1 nucleocapsid function: NMR solution structure determination of a ternary complex involving a 2:1 inhibitor/NC stoichiometry. *J. Mol. Biol.* **425**, 1982–98.
- (17) De Guzman, R. N., Wu, Z. R., Stalling, C. C., Pappalardo, L., Borer, P. N., and Summers, M. F. (1998) Structure of the HIV-1 nucleocapsid protein bound to the SL3 psi-RNA recognition element. *Science* **279**, 384–8.
- (18) Amarasinghe, G. K., De Guzman, R. N., Turner, R. B., and Summers, M. F. (2000) NMR structure of stem-loop SL2 of the HIV-1 psi RNA packaging signal reveals a novel A-U-A base-triple platform. *J. Mol. Biol.* **299**, 145–56.
- (19) Karn, J., and Graeble, M. A. (1992) New insights into the mechanism of HIV-1 trans-activation. *Trends Genet.* **8**, 365–8.
- (20) You, J. C., and McHenry, C. S. (1994) Human immunodeficiency virus nucleocapsid protein accelerates strand transfer of the terminally redundant sequences involved in reverse transcription. *J. Biol. Chem.* **269**, 31491–5.
- (21) Sosic, A., Frecentese, F., Perissutti, E., Sinigaglia, L., Santagada, V., Caliendo, G., Magli, E., Ciano, A., Zagotto, G., Parolin, C., et al. (2013) Design, synthesis and biological evaluation of TAR and cTAR binders as HIV-1 nucleocapsid inhibitors. *MedChemComm* **4**, 1388–1393.
- (22) Carlson, C. B., Vuysich, M., Gooch, B. D., and Beal, P. A. (2003) Preferred RNA binding sites for a threading intercalator revealed by in vitro evolution. *Chem. Biol.* **10**, 663–72.
- (23) Sosic, A., Cappellini, M., Scalabrin, M., and Gatto, B. (2015) Nucleocapsid Annealing-Mediated Electrophoresis (NAME) Assay Allows the Rapid Identification of HIV-1 Nucleocapsid Inhibitors. *J. Visualized Exp.*, e52474.
- (24) Zagotto, G., Ricci, A., Vasquez, E., Sandoli, A., Benedetti, S., Palumbo, M., and Sissi, C. (2011) Tuning G-quadruplex vs double-stranded DNA recognition in regioisomeric lysyl-peptidyl-anthraquinone conjugates. *Bioconjugate Chem.* **22**, 2126–35.
- (25) Shvadchak, V., Sanglier, S., Rocle, S., Villa, P., Haiech, J., Hibert, M., Van Dorsselaer, A., Mély, Y., and de Rocquigny, H. (2009) Identification by high throughput screening of small compounds inhibiting the nucleic acid destabilization activity of the HIV-1 nucleocapsid protein. *Biochimie* **91**, 916–923.
- (26) Sosic, A., Cappellini, M., Sinigaglia, L., Jacquet, R., Deffieux, D., Fabris, D., Quideau, S., and Gatto, B. (2015) Polyphenolic C-

glucosidic ellagitannins present in oak-aged wine inhibit HIV-1 nucleocapsid protein. *Tetrahedron* 71, 3020–3026.

(27) Beltz, H., Piemont, E., Schaub, E., Ficheux, D., Roques, B., Darlix, J. L., and Mely, Y. (2004) Role of the structure of the top half of HIV-1 cTAR DNA on the nucleic acid destabilizing activity of the nucleocapsid protein NCp7. *J. Mol. Biol.* 338, 711–23.

(28) Kanevsky, I., Chaminade, F., Chen, Y., Godet, J., Rene, B., Darlix, J. L., Mely, Y., Mauffret, O., and Fosse, P. (2011) Structural determinants of TAR RNA-DNA annealing in the absence and presence of HIV-1 nucleocapsid protein. *Nucleic Acids Res.* 39, 8148–62.

(29) Boudier, C., Storchak, R., Sharma, K. K., Didier, P., Follenius-Wund, A., Muller, S., Darlix, J. L., and Mely, Y. (2010) The mechanism of HIV-1 Tat-directed nucleic acid annealing supports its role in reverse transcription. *J. Mol. Biol.* 400, 487–501.

(30) Boudier, C., Humbert, N., Chaminade, F., Chen, Y., de Rocquigny, H., Godet, J., Mauffret, O., Fosse, P., and Mely, Y. (2014) Dynamic interactions of the HIV-1 Tat with nucleic acids are critical for Tat activity in reverse transcription. *Nucleic Acids Res.* 42, 1065–78.

(31) Nabel, G., and Baltimore, D. (1987) An inducible transcription factor activates expression of human immunodeficiency virus in T cells. *Nature* 326, 711–3.

(32) Berkhout, B., Silverman, R. H., and Jeang, K. T. (1989) Tat trans-activates the human immunodeficiency virus through a nascent RNA target. *Cell* 59, 273–82.

(33) Weeks, K. M., Ampe, C., Schltz, S. C., Steitz, T. A., and Crothers, D. M. (1990) Fragments of the HIV-1 Tat protein specifically bind TAR RNA. *Science* 249, 1281–1285.

(34) Rana, T. M., and Jeang, K. T. (1999) Biochemical and functional interactions between HIV-1 Tat protein and TAR RNA. *Arch. Biochem. Biophys.* 365, 175–85.

(35) Churcher, M. J., Lamont, C., Hamy, F., Dingwall, C., Green, S. M., Lowe, A. D., Butler, J. G., Gait, M. J., and Karn, J. (1993) High affinity binding of TAR RNA by the human immunodeficiency virus type-1 tat protein requires base-pairs in the RNA stem and amino acid residues flanking the basic region. *J. Mol. Biol.* 230, 90–110.

(36) Cao, H., Tamilarasu, N., and Rana, T. M. (2006) Orientation and affinity of HIV-1 Tat fragments in Tat-TAR complex determined by fluorescence resonance energy transfer. *Bioconjugate Chem.* 17, 352–8.

(37) Manfroni, G., Gatto, B., Tabarrini, O., Sabatini, S., Cecchetti, V., Giaretta, G., Parolin, C., del Vecchio, C., Calistri, A., Palumbo, M., et al. (2009) Synthesis and Biological Evaluation of 2-Phenylquinolones Targeted at Tat/TAR Recognition. *Bioorg. Med. Chem. Lett.* 19, 714–717.

(38) Tabarrini, O., Massari, S., Daelemans, D., Meschini, F., Manfroni, G., Bottega, L., Gatto, B., Palumbo, M., Pannecouque, C., and Cecchetti, V. (2010) Studies of anti-HIV transcription inhibitor quinolones: identification of potent N1-vinyl derivatives. *ChemMedChem* 5, 1880–92.

(39) Gooch, B. D., and Beal, P. A. (2004) Recognition of duplex RNA by helix-threading peptides. *J. Am. Chem. Soc.* 126, 10603–10.

(40) Scalabrin, M., Siu, Y., Asare-Okai, P. N., and Fabris, D. (2014) Structure-specific ribonucleases for MS-based elucidation of higher-order RNA structure. *J. Am. Soc. Mass Spectrom.* 25, 1136–45.

(41) McCauley, M. J., Rouzina, I., Manthei, K. A., Gorelick, R. J., Musier-Forsyth, K., and Williams, M. C. (2015) Targeted binding of nucleocapsid protein transforms the folding landscape of HIV-1 TAR RNA. *Proc. Natl. Acad. Sci. U. S. A.* 112, 13555–60.

(42) Rye, H. S., and Glazer, A. N. (1995) Interaction of dimeric intercalating dyes with single-stranded DNA. *Nucleic Acids Res.* 23, 1215–22.

(43) Wang, Z., and Rana, T. M. (1996) RNA conformation in the Tat-TAR complex determined by site-specific photo-cross-linking. *Biochemistry* 35, 6491–9.

(44) Wang, Z., and Rana, T. M. (1998) RNA-protein interactions in the Tat-trans-activation response element complex determined by site-specific photo-cross-linking. *Biochemistry* 37, 4235–43.

(45) Turner, K. B., Hagan, N. A., and Fabris, D. (2006) Inhibitory effects of archetypal nucleic acid ligands on the interactions of HIV-1 nucleocapsid protein with elements of Psi-RNA. *Nucleic Acids Res.* 34, 1305–16.

(46) Turner, K. B., Hagan, N. A., Kohlway, A. S., and Fabris, D. (2006) Mapping noncovalent ligand binding to stemloop domains of the HIV-1 packaging signal by tandem mass spectrometry. *J. Am. Soc. Mass Spectrom.* 17, 1402–11.

(47) Turner, K. B., Kohlway, A. S., Hagan, N. A., and Fabris, D. (2009) Noncovalent probes for the investigation of structure and dynamics of protein-nucleic acid assemblies: the case of NC-mediated dimerization of genomic RNA in HIV-1. *Biopolymers* 91, 283–96.

(48) Hagan, N., and Fabris, D. (2003) Direct mass spectrometric determination of the stoichiometry and binding affinity of the complexes between nucleocapsid protein and RNA stem-loop hairpins of the HIV-1 Psi-recognition element. *Biochemistry* 42, 10736–45.

(49) Fabris, D., Zaia, J., Hathout, Y., and Fenselau, C. (1996) Retention of Thiol Protons in Two Classes of Protein Zinc Ion Coordination Centers. *J. Am. Chem. Soc.* 118, 12242–12243.